

# Spectroscopy and Regge trajectories of heavy quarkonia and $B_c$ mesons

D. Ebert<sup>1</sup>, R. N. Faustov<sup>2</sup> and V. O. Galkin<sup>1,2</sup>

<sup>1</sup> *Institut für Physik, Humboldt-Universität zu Berlin,  
Newtonstr. 15, D-12489 Berlin, Germany*

<sup>2</sup> *Dorodnicyn Computing Centre, Russian Academy of Sciences,  
Vavilov Str. 40, 119991 Moscow, Russia*

The mass spectra of charmonia, bottomonia and  $B_c$  mesons are calculated in the framework of the QCD-motivated relativistic quark model based on the quasipotential approach. The dynamics of heavy quarks and antiquarks is treated fully relativistically without application of the nonrelativistic  $v^2/c^2$  expansion. The known one-loop radiative corrections to the heavy quark potential are taken into account perturbatively. The heavy quarkonium masses are calculated up to rather high orbital and radial excitations ( $L = 5$ ,  $n_r = 5$ ). On this basis the Regge trajectories are constructed both in the total angular momentum  $J$  and radial quantum number  $n_r$ . It is found that the daughter trajectories are almost linear and parallel, while parent trajectories exhibit some nonlinearity in the low mass region. Such nonlinearity is most pronounced for bottomonia and is only marginal for charmonia. The obtained results are compared with the available experimental data, and a possible interpretation of the new charmonium-like states above open charm production threshold is discussed.

PACS numbers: 14.40.Pq, 12.39.Ki

## I. INTRODUCTION

At present a vast amount of experimental data on the heavy quarkonium spectroscopy has been accumulated [1]. The number of known states is constantly increasing. Thus, in the last eight years more than ten new charmonium-like states have been discovered (for a recent review see e.g. [2]). The total number of charmonium states, listed in the Particle Data Group Listings [1], is 25 at present. Some of the new states (such as  $\eta_c(2S)$ ,  $h_c$ ,  $\chi_{c2}(2P)$ , etc.) are the long-awaited ones, expected by quark models many years ago, while some others, with masses higher than the threshold of the open charm production, have narrow widths and unexpected decay properties [2]. There are theoretical indications that some of these new states could be the first manifestation of the existence of exotic hadrons (tetraquarks, molecules, hybrids etc.), which are expected to exist in QCD (see e.g. [3] and references therein). In order to explore such options, a comprehensive understanding of the heavy quarkonium spectroscopy up to rather high orbital and radial excitations is required. The LHCb Collaboration at the Large Hadron Collider (LHC) [4] plans to search for the bottom counterparts of the newly discovered charmonium-like states [5]. At present, the experimentally known bottomonium spectrum consists of 14 states [1]. Moreover, new experimental data on the spectroscopy of  $B_c$  mesons are expected from LHC [6]. Therefore, the

investigation of the masses of the excited heavy quarkonia states represents an important and interesting problem. A reliable calculation of the masses of excited heavy quark-antiquark states will allow to single out experimental candidates for the exotic multi-quark states.

In Ref. [7] we calculated the mass spectra of charmonia, bottomonia and  $B_c$  mesons on the basis of a three-dimensional relativistic quasipotential wave equation with a QCD-motivated potential. For this calculation, a  $v^2/c^2$  expansion up to the second order was used. Masses of several lowest orbital and radial excitations were obtained, mainly for the states lying under the open flavour production threshold. This investigation indicated that the charm quark is not heavy enough to be considered as nonrelativistic, especially for excited states [7]. Therefore, a reliable consideration of the highly excited charmonium states requires a completely relativistic treatment of the charmed quark without an expansion in its velocity. In this paper we extend the approach previously used for the investigations of light meson spectroscopy [8], where relativistic quark dynamics was treated completely relativistically, to heavy quarkonia. Then the relativistic quasipotential, which determines the quark dynamics in heavy quarkonia, is an extremely non-local function in the coordinate space. In order to make it local, we replace the quark energies, entering the quark spinors, with the corresponding on-mass-shell energies. Such procedure makes the quasipotential local, but introduces a rather complicated nonlinear dependence on the bound state mass. The quasipotential equation with the complete relativistic potential can then be solved numerically using previously developed numerical methods [9]. In order to improve our description, leading radiative corrections to the heavy quark potential [10] are also taken into account. Such corrections are suppressed by additional powers of  $\alpha_s$ , which are rather small for heavy quarkonia, and are known only in the framework of the  $v^2/c^2$  expansion. Therefore we treat them perturbatively. The calculation of the masses of highly orbitally and radially excited states up to the fifth excitation is carried out. On this basis, the Regge trajectories for charmonia, bottomonia and  $B_c$  mesons can be constructed both in the total angular momentum  $J$  and radial quantum number  $n_r$ , and properties like linearity, parallelism and equidistance of these trajectories can be checked. There are reasons to expect that the parent Regge trajectories can be nonlinear due to the compactness of their ground and lowest excited states, which puts them in the region where both the linear confining and Coulomb parts of the quark-antiquark potential play an equally important role. Note also that the possibility of the assignment of the experimentally observed highly excited heavy quarkonium states to a particular Regge trajectory could help in determining their quantum numbers and elucidating their nature.

In recent papers [11, 12] we investigated the possible interpretation of some new unconventional charmonium-like states [2] as diquark-antidiquark tetraquarks. In particular, the relativistic dynamical calculation of the masses of such states was performed. Here we complement this study by calculating the spectrum of the highly excited conventional heavy quark-antiquark states in the same mass region. As a result, we will obtain a consistent picture of the recently discovered heavy quarkonium states within the same relativistic quark model.

A vast literature on the heavy quarkonium spectroscopy is now available. Therefore, we mostly refer to the recent comprehensive reviews [2, 13–15], where the references to earlier review and original papers can be found. Recent investigations of highly excited heavy quarkonium states and their Regge trajectories can be found, e.g., in Refs. [16–18]. For very recent unquenched lattice QCD calculations see, e.g., Ref. [19] and references therein.

## II. RELATIVISTIC QUARK MODEL

In the relativistic quark model based on the quasipotential approach a meson is described by the wave function of the bound quark-antiquark state, which satisfies the quasipotential equation of the Schrödinger type [7]

$$\left( \frac{b^2(M)}{2\mu_R} - \frac{\mathbf{p}^2}{2\mu_R} \right) \Psi_M(\mathbf{p}) = \int \frac{d^3q}{(2\pi)^3} V(\mathbf{p}, \mathbf{q}; M) \Psi_M(\mathbf{q}), \quad (1)$$

where the relativistic reduced mass is

$$\mu_R = \frac{E_1 E_2}{E_1 + E_2} = \frac{M^4 - (m_1^2 - m_2^2)^2}{4M^3}, \quad (2)$$

and  $E_1, E_2$  are given by

$$E_1 = \frac{M^2 - m_2^2 + m_1^2}{2M}, \quad E_2 = \frac{M^2 - m_1^2 + m_2^2}{2M}. \quad (3)$$

Here  $M = E_1 + E_2$  is the meson mass,  $m_{1,2}$  are the quark masses, and  $\mathbf{p}$  is their relative momentum. In the center-of-mass system the relative momentum squared on mass shell reads

$$b^2(M) = \frac{[M^2 - (m_1 + m_2)^2][M^2 - (m_1 - m_2)^2]}{4M^2}. \quad (4)$$

The kernel  $V(\mathbf{p}, \mathbf{q}; M)$  in Eq. (1) is the quasipotential operator of the quark-antiquark interaction. It is constructed with the help of the off-mass-shell scattering amplitude, projected onto the positive energy states. Constructing the quasipotential of the quark-antiquark interaction, we have assumed that the effective interaction is the sum of the usual one-gluon exchange term with the mixture of long-range vector and scalar linear confining potentials, where the vector confining potential contains the Pauli interaction. The quasipotential is then defined by

$$V(\mathbf{p}, \mathbf{q}; M) = \bar{u}_1(p) \bar{u}_2(-p) \mathcal{V}(\mathbf{p}, \mathbf{q}; M) u_1(q) u_2(-q), \quad (5)$$

with

$$\mathcal{V}(\mathbf{p}, \mathbf{q}; M) = \frac{4}{3} \alpha_s D_{\mu\nu}(\mathbf{k}) \gamma_1^\mu \gamma_2^\nu + V_{\text{conf}}^V(\mathbf{k}) \Gamma_1^\mu \Gamma_{2;\mu} + V_{\text{conf}}^S(\mathbf{k}),$$

where  $\alpha_s$  is the QCD coupling constant,  $D_{\mu\nu}$  is the gluon propagator in the Coulomb gauge,  $\gamma_\mu$  and  $u(p)$  are the Dirac matrices and spinors and  $\mathbf{k} = \mathbf{p} - \mathbf{q}$ .

The effective long-range vector vertex is given by

$$\Gamma_\mu(\mathbf{k}) = \gamma_\mu + \frac{i\kappa}{2m} \sigma_{\mu\nu} k^\nu, \quad (6)$$

where  $\kappa$  is the Pauli interaction constant characterizing the anomalous chromomagnetic moment of quarks. Vector and scalar confining potentials in the nonrelativistic limit reduce to

$$\begin{aligned} V_{\text{conf}}^V(r) &= (1 - \varepsilon)(Ar + B), \\ V_{\text{conf}}^S(r) &= \varepsilon(Ar + B), \end{aligned} \quad (7)$$

reproducing

$$V_{\text{conf}}(r) = V_{\text{conf}}^S(r) + V_{\text{conf}}^V(r) = Ar + B, \quad (8)$$

where  $\varepsilon$  is the mixing coefficient. Therefore, in this limit the Cornell-type potential is reproduced

$$V_{\text{NR}}(r) = -\frac{4}{3} \frac{\alpha_s}{r} + Ar + B. \quad (9)$$

All the model parameters have the same values as in our previous papers [7, 20]. The constituent quark masses  $m_u = m_d = 0.33$  GeV,  $m_s = 0.5$  GeV,  $m_c = 1.55$  GeV,  $m_b = 4.88$  GeV, and the parameters of the linear potential  $A = 0.18$  GeV<sup>2</sup> and  $B = -0.16$  GeV have the usual values of quark models. The value of the mixing coefficient of vector and scalar confining potentials  $\varepsilon = -1$  has been determined from the consideration of charmonium radiative decays [7] and matching heavy quark effective theory (HQET). Finally, the universal Pauli interaction constant  $\kappa = -1$  has been fixed from the analysis of the fine splitting of heavy quarkonia  $^3P_J$ -states [7]. In this case, the long-range chromomagnetic interaction of quarks, which is proportional to  $(1 + \kappa)$ , vanishes in accordance with the flux-tube model.

### III. QUARK-ANTIQUARK POTENTIAL

The investigations of the heavy quark dynamics in heavy mesons indicate that the charm quark is not heavy enough to be considered as nonrelativistic. Indeed, estimates of the averaged velocity squared for the ground-state charmonium give the value  $\langle v^2/c^2 \rangle \sim 0.25$ . For excited charmonium states the  $\langle v^2/c^2 \rangle$  values are even higher. Therefore, a reliable calculation of the charmonium spectroscopy requires a completely relativistic treatment of the charmed quark without an expansion in its velocity.

The quasipotential (5) can in principal be used for arbitrary quark masses. The substitution of the Dirac spinors into (5) results in an extremely nonlocal potential in the configuration space. Clearly, it is very hard to deal with such potentials without any additional approximations. In order to simplify the relativistic  $Q\bar{Q}$  potential, we make the following replacement in the Dirac spinors:

$$\epsilon_{1,2}(p) = \sqrt{m_{1,2}^2 + \mathbf{p}^2} \rightarrow E_{1,2} \quad (10)$$

(see the discussion of this point in [9, 20]). This substitution makes the Fourier transformation of the potential (5) local.

The resulting  $Q\bar{Q}$  potential then reads

$$V(r) = V_{\text{SI}}(r) + V_{\text{SD}}(r), \quad (11)$$

where the explicit expression for the spin-independent  $V_{\text{SI}}(r)$  can be found in Ref. [8]. The structure of the spin-dependent potential is given by

$$V_{\text{SD}}(r) = a \mathbf{L} \cdot \mathbf{S} + b \left[ \frac{3}{r^2} (\mathbf{S}_1 \cdot \mathbf{r})(\mathbf{S}_2 \cdot \mathbf{r}) - (\mathbf{S}_1 \cdot \mathbf{S}_2) \right] + c \mathbf{S}_1 \cdot \mathbf{S}_2 + d \mathbf{L} \cdot (\mathbf{S}_1 - \mathbf{S}_2) + e (\mathbf{L} \mathbf{S}_1)(\mathbf{L} \mathbf{S}_2), \quad (12)$$

where  $\mathbf{L}$  is the orbital angular momentum,  $\mathbf{S}_i$  is the quark spin,  $\mathbf{S} = \mathbf{S}_1 + \mathbf{S}_2$ . The coefficients  $a$ ,  $b$ ,  $c$ ,  $d$  and  $e$  are expressed through the corresponding derivatives of the Coulomb and confining potentials. Their explicit expressions are given in Ref. [8]. Since we also include the one-loop radiative corrections in our calculations, the strong coupling constant  $\alpha_s$  in the

static potential (9) should be replaced by the corrected constant  $\bar{\alpha}_V$  [10]:

$$\begin{aligned}\bar{\alpha}_V(\mu^2) &= \alpha_s(\mu^2) \left[ 1 + \left( \frac{a_1}{4} + \frac{\gamma_E \beta_0}{2} \right) \frac{\alpha_s(\mu^2)}{\pi} \right], \\ a_1 &= \frac{31}{3} - \frac{10}{9} n_f, \quad \beta_0 = 11 - \frac{2}{3} n_f,\end{aligned}\tag{13}$$

where  $n_f$  is the number of flavours,  $\mu$  is a renormalization scale and  $\gamma_E \cong 0.5772$  is the Euler constant.

The resulting quasipotential equation with the complete kernel (11) is solved numerically without any approximations. The remaining one-loop radiative corrections, which are not included in the renormalized coupling constant (13), are known only in the framework of the  $v/c$  expansion [10]; therefore we treat them perturbatively. The additional contributions are the following [7, 10]:

(a) to the spin-independent part

$$\begin{aligned}\delta V_{\text{SI}}(r) &= -\frac{4}{3} \frac{\beta_0 \alpha_s^2(\mu^2)}{2\pi} \frac{\ln(\mu r)}{r} + \frac{1}{8} \left( \frac{1}{m_1^2} + \frac{1}{m_2^2} \right) \Delta \left[ -\frac{4}{3} \frac{\beta_0 \alpha_s^2(\mu^2)}{2\pi} \frac{\ln(\mu r)}{r} \right] \\ &\quad + \frac{1}{2m_1 m_2} \left[ -\frac{4}{3} \frac{\beta_0 \alpha_s^2(\mu^2)}{2\pi} \left\{ \mathbf{p}^2 \frac{\ln(\mu r)}{r} + \frac{(\mathbf{p} \cdot \mathbf{r})^2}{r^2} \left( \frac{\ln(\mu r)}{r} - \frac{1}{r} \right) \right\} \right]_W,\end{aligned}\tag{14}$$

(b) to the spin-dependent part

$$\begin{aligned}\delta a &= \frac{1}{4} \left( \frac{1}{m_1^2} + \frac{1}{m_2^2} \right) \frac{4}{3} \frac{\alpha_s^2(\mu^2)}{\pi r^3} \left[ \frac{7}{3} - \frac{\beta_0}{12} + \gamma_E \left( \frac{\beta_0}{2} - 3 \right) + \frac{\beta_0}{2} \ln(\mu r) - 3 \ln(\sqrt{m_1 m_2} r) \right] \\ &\quad + \frac{1}{m_1 m_2} \frac{4}{3} \frac{\alpha_s^2(\mu^2)}{\pi r^3} \left[ \frac{1}{6} - \frac{\beta_0}{12} + \gamma_E \left( \frac{\beta_0}{2} - \frac{3}{2} \right) + \frac{\beta_0}{2} \ln(\mu r) - \frac{3}{2} \ln(\sqrt{m_1 m_2} r) \right] \\ &\quad + \left( \frac{1}{m_1^2} - \frac{1}{m_2^2} \right) \frac{\alpha_s^2(\mu^2)}{2\pi r^3} \ln \frac{m_2}{m_1},\end{aligned}\tag{15}$$

$$\delta b = \frac{1}{3m_1 m_2} \frac{4\alpha_s^2(\mu^2)}{\pi r^3} \left[ \frac{29}{6} - \frac{1}{4} \beta_0 + \gamma_E \left( \frac{\beta_0}{2} - 3 \right) + \frac{\beta_0}{2} \ln(\mu r) - 3 \ln(\sqrt{m_1 m_2} r) \right],\tag{16}$$

$$\begin{aligned}\delta c &= \frac{4}{3m_1 m_2} \frac{8\pi \alpha_s^2(\mu^2)}{3\pi} \left\{ \left( \frac{5}{12} \beta_0 - \frac{11}{3} - \left[ \frac{m_1 - m_2}{m_1 + m_2} + \frac{1}{8} \frac{m_1 + m_2}{m_1 - m_2} \right] \ln \frac{m_2}{m_1} \right) \delta^3(r) \right. \\ &\quad \left. + \left[ -\frac{\beta_0}{8\pi} \nabla^2 \left( \frac{\ln(\mu r) + \gamma_E}{r} \right) + \frac{21}{16\pi} \nabla^2 \left( \frac{\ln(\sqrt{m_1 m_2} r) + \gamma_E}{r} \right) \right] \right\},\end{aligned}\tag{17}$$

$$\begin{aligned}\delta d &= \frac{1}{4} \left( \frac{1}{m_1^2} - \frac{1}{m_2^2} \right) \frac{4}{3} \frac{\alpha_s^2(\mu^2)}{\pi r^3} \left[ \frac{7}{3} - \frac{\beta_0}{12} + \gamma_E \left( \frac{\beta_0}{2} - 3 \right) + \frac{\beta_0}{2} \ln(\mu r) - 3 \ln(\sqrt{m_1 m_2} r) \right] \\ &\quad + \left( \frac{1}{m_1} + \frac{1}{m_2} \right)^2 \frac{\alpha_s^2(\mu^2)}{2\pi r^3} \ln \frac{m_2}{m_1},\end{aligned}\tag{18}$$

where for quantities quadratic in the momenta we use the Weyl ordering prescription [21]:

$$\{f(r) p^i p^j\}_W = \frac{1}{4} \{ \{f(r), p^i\}, p^j \}.$$

Since we consider only heavy quarks, for the dependence of the QCD coupling constant  $\alpha_s(\mu^2)$  on the renormalization point  $\mu^2$  we use the leading order result

$$\alpha_s(\mu^2) = \frac{4\pi}{\beta_0 \ln(\mu^2/\Lambda^2)}. \quad (19)$$

In our numerical calculations we set the renormalization scale  $\mu = 2m_1m_2/(m_1 + m_2)$  and  $\Lambda = 0.169$  GeV, which gives  $\alpha_s = 0.315$  for  $m_1 = m_2 = m_c$  (charmonium);  $\alpha_s = 0.224$  for  $m_1 = m_2 = m_b$  (bottomonium); and  $\alpha_s = 0.286$  for  $m_1 = m_c, m_2 = m_b$  ( $B_c$  meson).<sup>1</sup>

For the equal mass case ( $m_1 = m_2 = m$ ) the contribution of the annihilation diagrams

$$\delta c' = \frac{8\alpha_s^2(\mu^2)}{3m^2} \left( \frac{4}{3} - \ln 2 \right) \delta^3(r), \quad (20)$$

which is of second order in  $\alpha_s$ , must be added to the spin-spin interaction coefficient  $\delta c$  in Eq. (17).

Moreover, for the calculation of the bottomonium mass spectrum it is also necessary to take into account additional one-loop corrections due to the finite mass of the charm quark [22]. We considered these corrections within our model in Ref. [23] and found that they give contributions of a few MeV and weakly depend on the quantum numbers of the bottomonium states. The one-loop correction to the static  $Q\bar{Q}$  potential in QCD due to the finite  $c$  quark mass is given by [22, 23]

$$\Delta V(r, m_c) = -\frac{4}{9} \frac{\alpha_s^2(\mu)}{\pi r} [\ln(\sqrt{a_0} m_c r) + \gamma_E + E_1(\sqrt{a_0} m_c r)], \quad (21)$$

where

$$E_1(x) = \int_x^\infty e^{-t} \frac{dt}{t} = -\gamma_E - \ln x - \sum_{n=1}^\infty \frac{(-x)^n}{n \cdot n!},$$

and  $a_0 = 5.2$ .

## IV. RESULTS AND DISCUSSION

### A. Calculation of the masses

We solve the quasipotential equation with the quasipotential (11), which nonperturbatively accounts for the relativistic dynamics of both heavy quarks, numerically. Then we add the one-loop radiative corrections (14)-(20) and the additional one-loop correction for bottomonium due to the finite mass of the charmed quark (21) by using perturbation theory. The calculated masses of charmonia, bottomonia and the  $B_c$  meson are given in Tables I-III, where  $n = n_r + 1$ ,  $n_r$  is the radial quantum number,  $L$ ,  $S$  and  $J$  are the quantum numbers of the orbital, spin and total angular momenta, respectively. They are confronted with available experimental data from PDG [1]. Good agreement of our predictions and data is found. It is important to note that the nonperturbative relativistic treatment gives a better

---

<sup>1</sup> Note that these values of  $\alpha_s(\mu^2)$  were fixed in Ref. [7] to optimize the fine and hyperfine splittings in charmonium and bottomonium (cf. Tables I, II).

TABLE I: Charmonium mass spectrum (in MeV).

State		Theory	Experiment [1]		State		Theory	Experiment [1]	
$n^{2S+1}L_J$	$J^{PC}$		meson	mass	$n^{2S+1}L_J$	$J^{PC}$		meson	mass
$1^1S_0$	$0^{-+}$	2981	$\eta_c(1S)$	2980.3(1.2)	$2^3D_1$	$1^{--}$	4150	$\psi(4160)$	4153(3)
$1^3S_1$	$1^{--}$	3096	$J/\psi(1S)$	3096.916(11)	$2^3D_2$	$2^{--}$	4190		
$2^1S_0$	$0^{-+}$	3635	$\eta_c(2S)$	3637(4)	$2^3D_3$	$3^{--}$	4220		
$2^3S_1$	$1^{--}$	3685	$\psi(2S)$	3686.09(4)	$2^1D_2$	$2^{-+}$	4196	$X(4160)?$	4156( $^{29}_{25}$ )
$3^1S_0$	$0^{-+}$	3989			$3^3D_1$	$1^{--}$	4507		
$3^3S_1$	$1^{--}$	4039	$\psi(4040)$	4039(1)	$3^3D_2$	$2^{--}$	4544		
$4^1S_0$	$0^{-+}$	4401			$3^3D_3$	$3^{--}$	4574		
$4^3S_1$	$1^{--}$	4427	$\psi(4415)$	4421(4)	$3^1D_2$	$2^{-+}$	4549		
$5^1S_0$	$0^{-+}$	4811			$4^3D_1$	$1^{--}$	4857		
$5^3S_1$	$1^{--}$	4837			$4^3D_2$	$2^{--}$	4896		
$6^1S_0$	$0^{-+}$	5155			$4^3D_3$	$3^{--}$	4920		
$6^3S_1$	$1^{--}$	5167			$4^1D_2$	$2^{-+}$	4898		
$1^3P_0$	$0^{++}$	3413	$\chi_{c0}(1P)$	3414.75(31)	$1^3F_2$	$2^{++}$	4041		
$1^3P_1$	$1^{++}$	3511	$\chi_{c1}(1P)$	3510.66(7)	$1^3F_3$	$3^{++}$	4068		
$1^3P_2$	$2^{++}$	3555	$\chi_{c2}(1P)$	3556.20(9)	$1^3F_4$	$4^{++}$	4093		
$1^1P_1$	$1^{+-}$	3525	$h_c(1P)$	3525.41(16)	$1^1F_3$	$3^{+-}$	4071		
$2^3P_0$	$0^{++}$	3870			$2^3F_2$	$2^{++}$	4361		
$2^3P_1$	$1^{++}$	3906			$2^3F_3$	$3^{++}$	4400		
$2^3P_2$	$2^{++}$	3949	$\chi_{c2}(2P)$	3927.2(2.6)	$2^3F_4$	$4^{++}$	4434		
$2^1P_1$	$1^{+-}$	3926			$2^1F_3$	$3^{+-}$	4406		
$3^3P_0$	$0^{++}$	4301			$1^3G_3$	$3^{--}$	4321		
$3^3P_1$	$1^{++}$	4319			$1^3G_4$	$4^{--}$	4343		
$3^3P_2$	$2^{++}$	4354	$X(4350)?$	4351(5)	$1^3G_5$	$5^{--}$	4357		
$3^1P_1$	$1^{+-}$	4337			$1^1G_4$	$4^{-+}$	4345		
$4^3P_0$	$0^{++}$	4698			$1^3H_4$	$4^{++}$	4572		
$4^3P_1$	$1^{++}$	4728			$1^3H_5$	$5^{++}$	4592		
$4^3P_2$	$2^{++}$	4763			$1^3H_6$	$6^{++}$	4608		
$4^1P_1$	$1^{+-}$	4744			$1^3H_5$	$5^{+-}$	4594		
$1^3D_1$	$1^{--}$	3783	$\psi(3770)$	3772.92(35)					
$1^3D_2$	$2^{--}$	3795							
$1^3D_3$	$3^{--}$	3813							
$1^1D_2$	$2^{-+}$	3807							

agreement with data than our previous heavy quarkonium mass spectrum calculation [7], where only relativistic corrections up to  $v^2/c^2$  order were taken into account. However, the differences between former and new predictions are rather small for most of the low-lying states and become noticeable only for higher excitations, where relativistic effects turn out to be particularly important.

The  $B_c$  meson states with  $J = L$ , given in Tables III, are mixtures of spin-triplet  $|^3L_L\rangle$

TABLE II: Bottomonium mass spectrum (in MeV).

State		Theory	Experiment [1]		State		Theory
$n^{2S+1}L_J$	$J^{PC}$		meson	mass	$n^{2S+1}L_J$	$J^{PC}$	
$1^1S_0$	$0^{-+}$	9398	$\eta_b(1S)$	9390.9(2.8)	$2^3D_1$	$1^{--}$	10435
$1^3S_1$	$1^{--}$	9460	$\Upsilon(1S)$	9460.30(26)	$2^3D_2$	$2^{--}$	10443
$2^1S_0$	$0^{-+}$	9990			$2^3D_3$	$3^{--}$	10449
$2^3S_1$	$1^{--}$	10023	$\Upsilon(2S)$	10023.26(31)	$2^1D_2$	$2^{-+}$	10445
$3^1S_0$	$0^{-+}$	10329			$3^3D_1$	$1^{--}$	10704
$3^3S_1$	$1^{--}$	10355	$\Upsilon(3S)$	10355.2(5)	$3^3D_2$	$2^{--}$	10711
$4^1S_0$	$0^{-+}$	10573			$3^3D_3$	$3^{--}$	10717
$4^3S_1$	$1^{--}$	10586	$\Upsilon(4S)$	10579.4(1.2)	$3^1D_2$	$2^{-+}$	10713
$5^1S_0$	$0^{-+}$	10851			$4^3D_1$	$1^{--}$	10949
$5^3S_1$	$1^{--}$	10869	$\Upsilon(10860)$	10876(1)	$4^3D_2$	$2^{--}$	10957
$6^1S_0$	$0^{-+}$	11061			$4^3D_3$	$3^{--}$	10963
$6^3S_1$	$1^{--}$	11088	$\Upsilon(11020)$	11019(8)	$4^1D_2$	$2^{-+}$	10959
$1^3P_0$	$0^{++}$	9859	$\chi_{b0}(1P)$	9859.44(52)	$1^3F_2$	$2^{++}$	10343
$1^3P_1$	$1^{++}$	9892	$\chi_{b1}(1P)$	9892.78(40)	$1^3F_3$	$3^{++}$	10346
$1^3P_2$	$2^{++}$	9912	$\chi_{b2}(1P)$	9912.21(40)	$1^3F_4$	$4^{++}$	10349
$1^1P_1$	$1^{+-}$	9900	$h_b(1P)$	9898.25(1.50)	$1^1F_3$	$3^{+-}$	10347
$2^3P_0$	$0^{++}$	10233	$\chi_{b0}(2P)$	10232.5(6)	$2^3F_2$	$2^{++}$	10610
$2^3P_1$	$1^{++}$	10255	$\chi_{b1}(2P)$	10255.46(55)	$2^3F_3$	$3^{++}$	10614
$2^3P_2$	$2^{++}$	10268	$\chi_{b2}(2P)$	10268.65(55)	$2^3F_4$	$4^{++}$	10617
$2^1P_1$	$1^{+-}$	10260	$h_b(2P)$	10259.76(1.57)	$2^1F_3$	$3^{+-}$	10615
$3^3P_0$	$0^{++}$	10521			$1^3G_3$	$3^{--}$	10511
$3^3P_1$	$1^{++}$	10541			$1^3G_4$	$4^{--}$	10512
$3^3P_2$	$2^{++}$	10550			$1^3G_5$	$5^{--}$	10514
$3^1P_1$	$1^{+-}$	10544			$1^1G_4$	$4^{-+}$	10513
$4^3P_0$	$0^{++}$	10781			$1^3H_4$	$4^{++}$	10670
$4^3P_1$	$1^{++}$	10802			$1^3H_5$	$5^{++}$	10671
$4^3P_2$	$2^{++}$	10812			$1^3H_6$	$6^{++}$	10672
$4^1P_1$	$1^{+-}$	10804			$1^3H_5$	$5^{+-}$	10671
$1^3D_1$	$1^{--}$	10154					
$1^3D_2$	$2^{--}$	10161	$\Upsilon(1D)$	10163.7(1.4)			
$1^3D_3$	$3^{--}$	10166					
$1^1D_2$	$2^{-+}$	10163					

and spin-singlet  $|^1L_L\rangle$  states:

$$\begin{aligned}
|\Psi_J\rangle &= |^1L_L\rangle \cos\theta + |^3L_L\rangle \sin\theta, \\
|\Psi'_J\rangle &= -|^1L_L\rangle \sin\theta + |^3L_L\rangle \cos\theta, \quad J = L = 1, 2, 3 \dots
\end{aligned} \tag{22}$$

where  $\theta$  is a mixing angle, and the primed state has the heavier mass. Such mixing occurs due to the nondiagonal spin-orbit and tensor terms in Eq. (12). The masses of physical



TABLE III:  $B_c$  meson mass spectrum (in MeV).

State		Theory	Experiment [1]		State		Theory
$n^{2S+1}L_J$	$J^P$		meson	mass	$n^{2S+1}L_J$	$J^P$	
$1^1S_0$	$0^-$	6272	$B_c$	6277(6)	$1^3D_1$	$1^-$	7021
$1^3S_1$	$1^-$	6333			$1D_2$	$2^-$	7025
$2^1S_0$	$0^-$	6842			$1D_2$	$2^-$	7026
$2^3S_1$	$1^-$	6882			$1^3D_3$	$3^-$	7029
$3^1S_0$	$0^-$	7226			$2^3D_1$	$1^-$	7392
$3^3S_1$	$1^-$	7258			$2D_2$	$2^-$	7399
$4^1S_0$	$0^-$	7585			$2D_2$	$2^-$	7400
$4^3S_1$	$1^-$	7609			$2^3D_3$	$3^-$	7405
$5^1S_0$	$0^-$	7928			$3^3D_1$	$1^-$	7732
$5^3S_1$	$1^-$	7947			$3D_2$	$2^-$	7741
$1^3P_0$	$0^+$	6699			$3D_2$	$2^-$	7743
$1P_1$	$1^+$	6743			$3^3D_3$	$3^-$	7750
$1P_1$	$1^+$	6750			$1^3F_2$	$2^+$	7273
$1^3P_2$	$2^+$	6761			$1F_3$	$3^+$	7269
$2^3P_0$	$0^+$	7094			$1F_3$	$3^+$	7268
$2P_1$	$1^+$	7134			$1^3F_4$	$4^+$	7277
$2P_1$	$1^+$	7147			$2^3F_2$	$2^+$	7618
$2^3P_2$	$2^+$	7157			$2F_3$	$3^+$	7616
$3^3P_0$	$0^+$	7474			$2F_3$	$3^+$	7615
$3P_1$	$1^+$	7500			$2^3F_4$	$4^{+-}$	7617
$3P_1$	$1^+$	7510			$1^3G_3$	$3^-$	7497
$3^3P_2$	$2^+$	7524			$1G_4$	$4^-$	7489
$4^3P_0$	$0^+$	7817			$1G_4$	$4^-$	7487
$4P_1$	$1^+$	7844			$1^3G_5$	$5^-$	7482
$4P_1$	$1^+$	7853			$2G_4$	$4^-$	7819
$4^3P_2$	$2^+$	7867			$2^3G_5$	$5^-$	7817

states were obtained by diagonalizing the mixing matrix. The obtained values of the mixing angles  $\theta$  are close to the ones given in Ref. [7].

## B. Regge trajectories

In our analysis we calculated masses of both orbitally and radially excited heavy quarkonia up to rather high excitation numbers ( $L = 5$  and  $n_r = 5$ ). This makes it possible to construct the Regge trajectories in the  $(J, M^2)$  and  $(n_r, M^2)$  planes using the following definitions:

a)  $(J, M^2)$  Regge trajectory:

$$J = \alpha M^2 + \alpha_0; \quad (23)$$

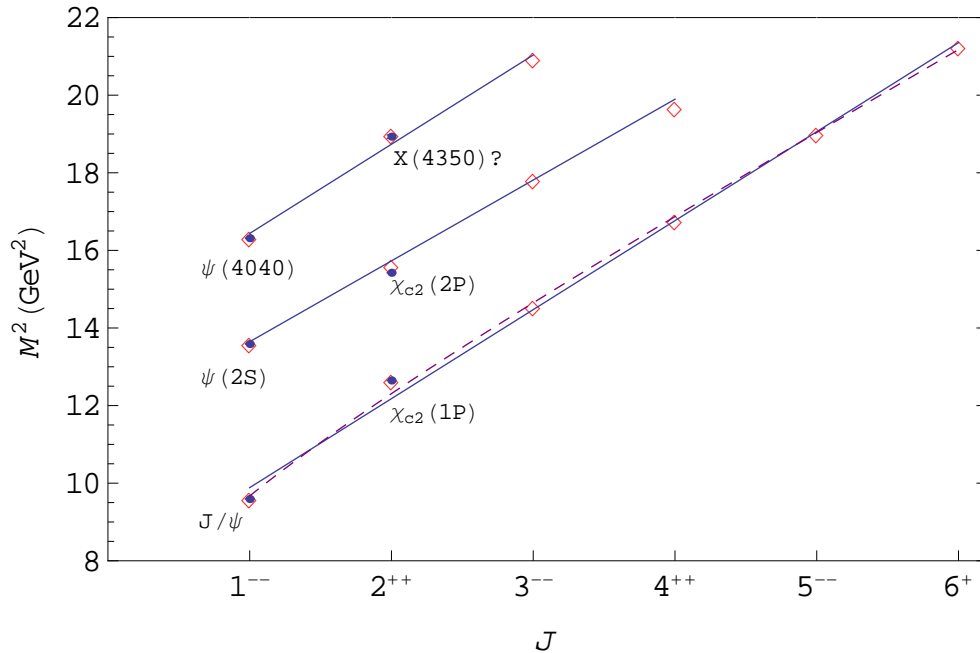


FIG. 1: Parent and daughter  $(J, M^2)$  Regge trajectories for charmonium states with natural parity ( $P = (-1)^J$ ). Diamonds are predicted masses. Available experimental data are given by dots with particle names. The dashed line corresponds to a nonlinear fit for the parent trajectory.

b)  $(n_r, M^2)$  Regge trajectory:

$$n_r = \beta M^2 + \beta_0, \quad (24)$$

where  $\alpha, \beta$  are the slopes and  $\alpha_0, \beta_0$  are the intercepts. The relations (23) and (24) arise in most models of quark confinement, but with different values of the slopes.

In Figs. 1-10 we plot the Regge trajectories in the  $(J, M^2)$  and  $(n_r, M^2)$  planes for charmonia, bottomonia and  $B_c$  mesons. The masses calculated in our model are shown by diamonds. Available experimental data are given by dots with error bars and corresponding meson names. Straight lines were obtained by the  $\chi^2$  fits of the calculated values. The fitted slopes and intercepts of the Regge trajectories are given in Tables IV and V. We see that the calculated charmonium masses fit nicely to the linear trajectories in both planes (maybe with the exception of the parent trajectories, where the  $J/\psi$  and  $\eta_c$  mesons seem to have slightly lower masses). These trajectories are almost parallel and equidistant. In the bottomonium and  $B_c$  meson sectors the situation is more complicated. The daughter trajectories, which involve both radially and orbitally excited states, turn out to be almost linear. On the other hand, the parent trajectories, which start from ground states, are exhibiting a nonlinear behaviour in the lower mass (excitation) region. Such nonlinearity is more pronounced in bottomonium. The origin of this nonlinearity can be easily understood, if one compares the mean radii of these states. The values of the mean square radii  $\sqrt{\langle r^2 \rangle}$  of charmonia,  $B_c$  mesons and bottomonia, calculated in our model, are given in Table VI. The static potential of the quark-antiquark interaction is plotted in Fig. 11 (solid line). In this figure we also separately plot the contributions from linear confinement (dashed line) and of the modulus of the Coulomb potential (dotted line). As seen from Fig. 11, the Coulomb potential dominates for distances less than 0.15 fm, while the confining potential is dominant

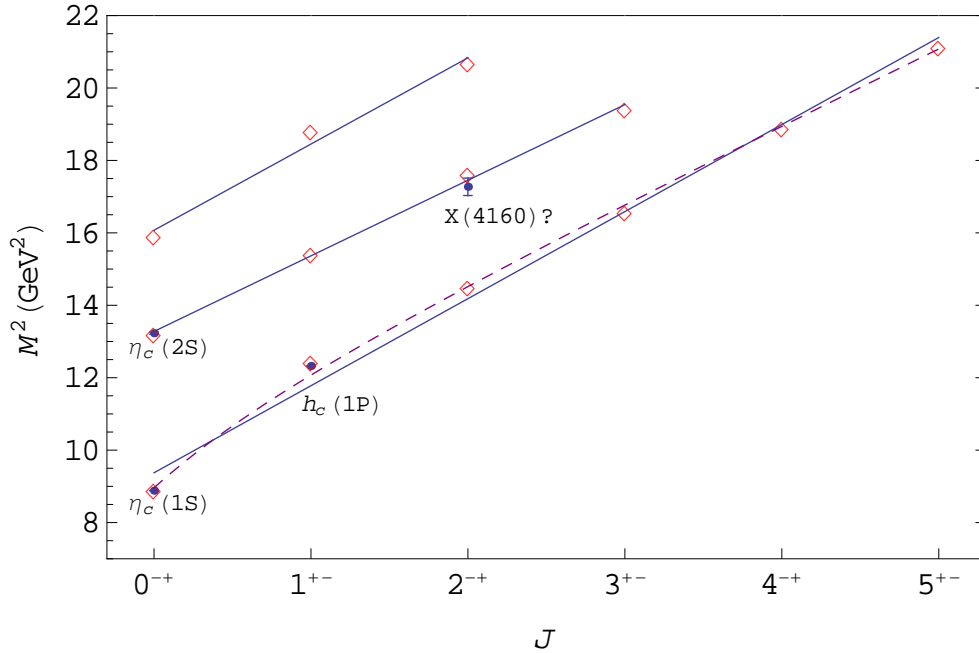


FIG. 2: Same as in Fig. 1 for charmonium states with unnatural parity ( $P = (-1)^{J+1}$ ).

for distances larger than 0.5 fm. In the intermediate region both potentials play an equally important role. Therefore the light mesons and charmonia (with the exception of the  $\eta_c$  and  $J/\psi$  which are in the intermediate region) have characteristic sizes which belong to the region, where the confining potential dominates in the interquark potential (9). This leads to the emergence of the linear Regge trajectories. Contrary, the ground and few first excited states of bottomonia and  $B_c$  mesons have smaller sizes and fall into the region, where the Coulomb part of the potential (9) gives an important contribution. As a result, the parent Regge trajectories of bottomonia and  $B_c$  mesons are nonlinear, while the daughter trajectories (which fall into the region, where the confining potential is dominant) are still linear ones. In Refs. [16, 24] an interpolating formula between the limiting cases of pure Coulomb and linear interactions was proposed. It can be written as follows:

(a) for the parent trajectory in the  $(J, M^2)$  plane

$$M^2 = \left( J - \frac{\gamma_1}{(J+2)^2} + \gamma_0 \right) / \gamma, \quad (25)$$

(b) for the  $J = 1$  trajectory in the  $(n_r, M^2)$  plane

$$M^2 = \left( n_r - \frac{\tau_1}{(n_r+2)^2} + \tau_0 \right) / \tau, \quad (26)$$

where the parameters  $\gamma$ ,  $\tau$ ,  $\gamma_0$ ,  $\tau_0$  and  $\gamma_1$ ,  $\tau_1$  determine the slopes, intercepts and nonlinearity of the Regge trajectories, respectively. Their fitted values are given in Table VII. The corresponding Regge trajectories are plotted in Figs. 1-10 by dashed lines. It is found that these nonlinear trajectories have the same slope  $\gamma$  for the given quarkonium family, which is generally in agreement (but slightly higher) with the linear trajectory slopes  $\alpha$  for the

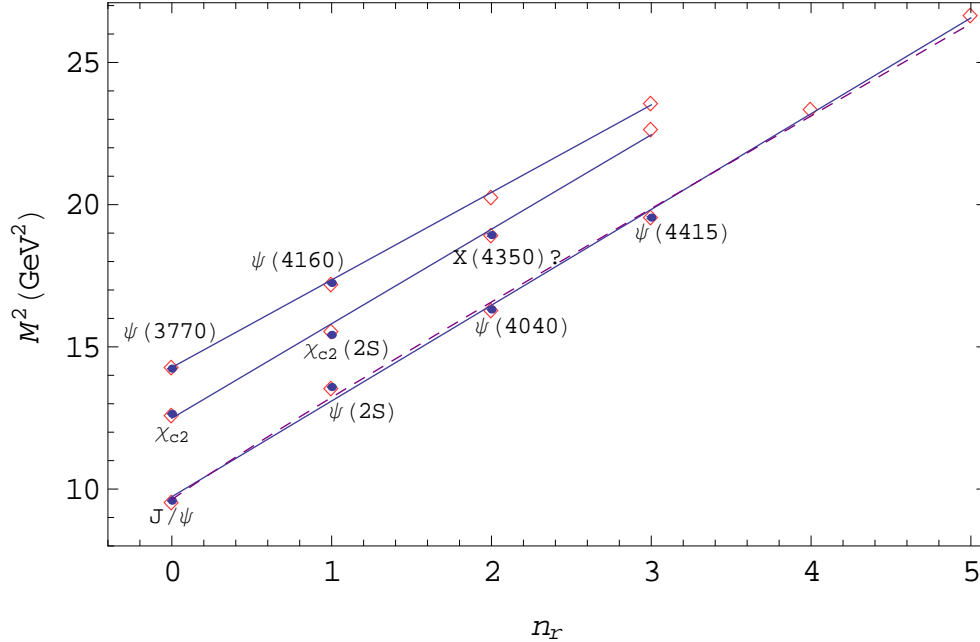


FIG. 3: The  $(n_r, M^2)$  Regge trajectories for vector ( $S$ -wave), tensor and vector ( $D$ -wave) charmonium states (from bottom to top). Notations are the same as in Fig. 1.

respective daughter trajectories given in Table IV. We see that the nonlinearity of the charmonium Regge trajectories is almost negligible, and its account does not significantly improve the quality of the fit compared to the linear one.

We can compare the slopes of linear Regge trajectories for heavy quarkonia obtained in this paper with our previous results for the slopes of Regge trajectories of light [8] and heavy-light [25] mesons. Such comparison shows that the slopes decrease rather fast with the growth of the quark masses: the slope  $\alpha$  decreases from about  $1.1 \text{ GeV}^{-2}$  for light mesons, composed from  $u, d$  quarks and antiquarks, to about  $0.24 \text{ GeV}^{-2}$  for bottomonium. However, the difference between slopes of heavy-light ( $Q\bar{q}$ ) mesons and of heavy quarkonia ( $Q\bar{Q}'$ ) is not so dramatic. In fact, comparing the present Tables IV, V and the corresponding Tables 4, 5 of Ref. [25], we see that the slopes for charmonia and  $D, D_s$  mesons have very close values, and the same is true also for bottomonia,  $B_c$  and  $B, B_s$  mesons. This might indicate that the slope of the meson Regge trajectory is mainly determined by the mass of the heaviest quark  $m_Q$ . The dependence of the Regge slopes  $\alpha$  and  $\beta$  on  $m_Q$  has in both planes with rather good accuracy the same simple form:  $\alpha, \beta \propto 1/\sqrt{m_Q}$ .

From the comparison of the slopes in Tables IV, V we see that the  $\alpha$  values are systematically larger than the  $\beta$  ones. The ratio of their mean values is about 1.4 for charmonia, bottomonia and  $B_c$  mesons. This value of the ratio is the same as for the charmed and bottom mesons [25], but slightly larger than for light mesons [8], for which  $\alpha/\beta$  was found to be about 1.3.

### C. Comparison with experiment

In Tables I-III we compare our predictions for the heavy quarkonium masses with the available experimental data [1]. We find that all states below the open flavour production

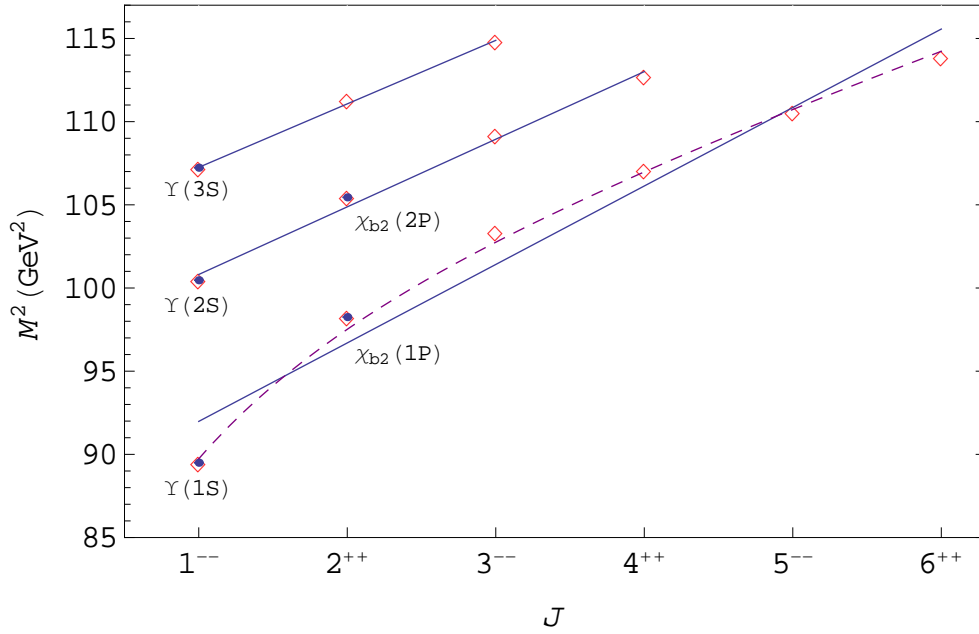


FIG. 4: Same as in Fig. 1 for bottomonium states with natural parity.

thresholds are well described by our model, the difference between predicted and measured masses does not exceed a few MeV. For higher excited states, which are above this threshold, most of the well-established conventional states (believed to be quark-antiquark ones) are also well described by our model, the difference between theory and experiment being somewhat larger, but it still does not exceed 20 MeV.<sup>2</sup> As it is seen from Figs. 1-10, these states fit to the corresponding Regge trajectories both in the  $(J, M^2)$  and  $(n_r, M^2)$  planes.

We first discuss the recently found quarkonium states below the open flavour production threshold. The observation and measurement of the mass of the pseudoscalar ground state  $\eta_b$  [28] provides a significant information about the spin-spin interaction in heavy quarkonia. The averaged bottomonium hyperfine splitting measured in  $\Upsilon(3S) \rightarrow \eta_b(1S)\gamma$  and  $\Upsilon(2S) \rightarrow \eta_b(1S)\gamma$  decays is  $\Delta M_{\text{hfs}}(\eta_b) \equiv M_{\Upsilon(1S)} - M_{\eta_b(1S)} = 69.3 \pm 2.8$  MeV [1, 28]. Very recently the Belle Collaboration [29] reported the first observation of the radiative transition  $h_b(1P) \rightarrow \eta_b(1S)\gamma$ . The measured  $\eta_b(1S)$  mass is  $9401.0 \pm 1.9^{+1.4}_{-2.4}$  MeV and the hyperfine splitting  $\Delta M_{\text{hfs}}(\eta_b) = 59.3 \pm 1.9^{+2.4}_{-1.4}$  MeV [29]. Our prediction for this splitting,  $\Delta M_{\text{hfs}}(\eta_b) = 62$  MeV, is in good agreement with the experimental values.<sup>3</sup> Note that our model correctly predicts the branching ratios of the corresponding radiative decays [7]. For the better understanding of the hyperfine interaction in heavy mesons it will be very interesting to measure the mass of the vector  $B_c^*$ -meson, which consists of two heavy quarks of different flavours, and

<sup>2</sup> Note that hadron loop effects [26, 27] can lead to mass shifts and state mixings. As shown in Ref. [27], the loop mass shifts can be absorbed by a change of the valence quark model parameters. However, the opening of the new threshold could provide a larger mass shifts to the nearby quarkonium states.

<sup>3</sup> Almost the same value of  $\Delta M_{\text{hfs}}(\eta_b) = 60$  MeV was predicted by us in Ref. [7], while most of other theoretical predictions, especially the ones based on perturbative calculations, gave significantly lower central values, e.g.,  $41 \pm 14$  MeV [30].

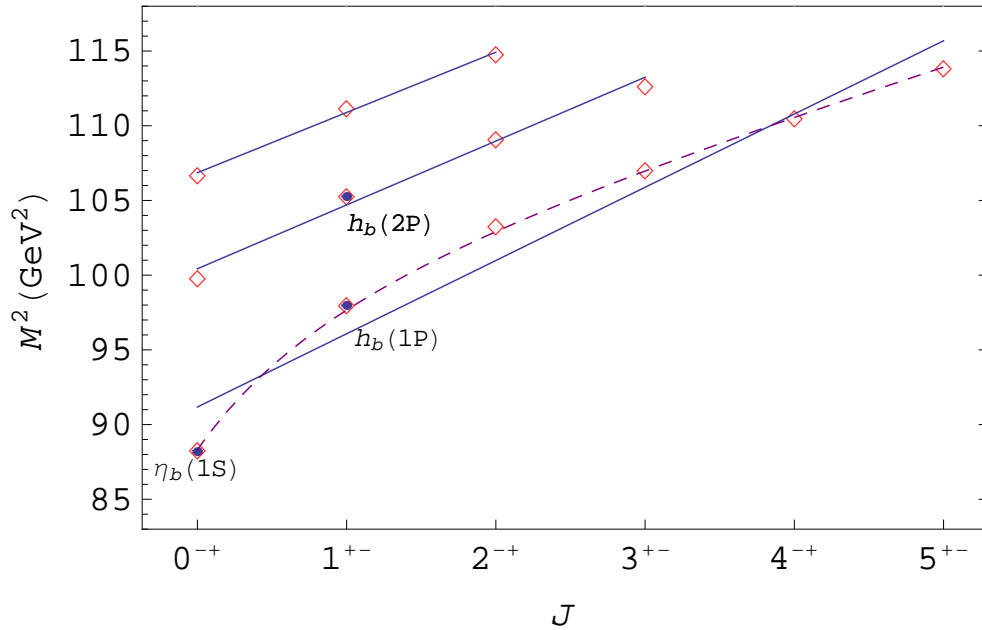


FIG. 5: Same as in Fig. 1 for bottomonium states with unnatural parity.

determine the related hyperfine splitting. Our model correctly predicts the pseudoscalar  $B_c$  meson mass and gives for the hyperfine splitting the value of  $\Delta M_{\text{hf}}(B_c) = 61$  MeV. Note that the LHCb Collaboration very recently measured the  $B_c$  meson mass, and their preliminary result is  $M(B_c^+) = 6268.0 \pm 4.0(\text{stat}) \pm 0.6(\text{syst})$  MeV, leading to the improved average  $M(B_c^+)^{\text{exp}} = 6272.95 \pm 5.17$  MeV [6].

Another important experimental test of the structure of the spin splittings in heavy quarkonia comes from the measurement of the masses of the spin-singlet  $P$ -levels first in charmonium  $h_c(1P)$  [31] and very recently in bottomonium  $h_b(1P)$  and  $h_b(2P)$  [32]. The measured masses of these states almost coincide with the spin-averaged centroid of the triplet states  $\langle M(^3P_J) \rangle = [M(\chi_{Q0}) + 3M(\chi_{Q1}) + 5M(\chi_{Q2})]/9$ . The hyperfine mass splittings  $\Delta M_{\text{hfs}}(nP) \equiv \langle M(n^3P_J) \rangle - M(n^1P_1)$  in bottomonium are found to be  $\Delta M_{\text{hfs}}(1P) = (1.62 \pm 1.52)$  MeV and  $\Delta M_{\text{hfs}}(2P) = (0.48^{+1.57}_{-1.22})$  MeV [32]. This observation indicates that the spin-spin contribution is negligible for  $P$ -levels, and thus shows the vanishing of the long-range chromomagnetic interaction in heavy quarkonia. In our model this is the result of the choice of the value of the long-range chromomagnetic quark moment  $\kappa = -1$ . Note that our original predictions [7] for the spin-singlet masses are confirmed by these measurements.

The recently observed  $\Upsilon(1^3D_2)$  state is the only  $D$ -wave state found below the threshold of open flavour production. Our prediction for its mass is consistent with the measured value. It will be interesting to observe other  $\Upsilon(1D)$  states in order to test further our understanding of spin-orbit and spin-spin interactions in heavy quarkonia.

Next we discuss the observed states above the open flavour production threshold. The most well-established states are the vector  $1^{--}$  states. For charmonium PDG [1] lists seven such states:  $\psi(3770)$ ,  $\psi(4040)$ ,  $\psi(4160)$ ,  $X(4260)$ ,  $X(4360)$ ,  $\psi(4415)$  and  $X(4660)$ , from which only the  $\psi$  states are included in the PDG Summary Tables [1]. These states are believed to be ordinary  $c\bar{c}$  charmonium (with isospin  $I = 0$ ). They are well described by our model (see Table I):  $\psi(4040)$  and  $\psi(4415)$  are the  $3^3S_1$  and  $4^3S_1$  states, while

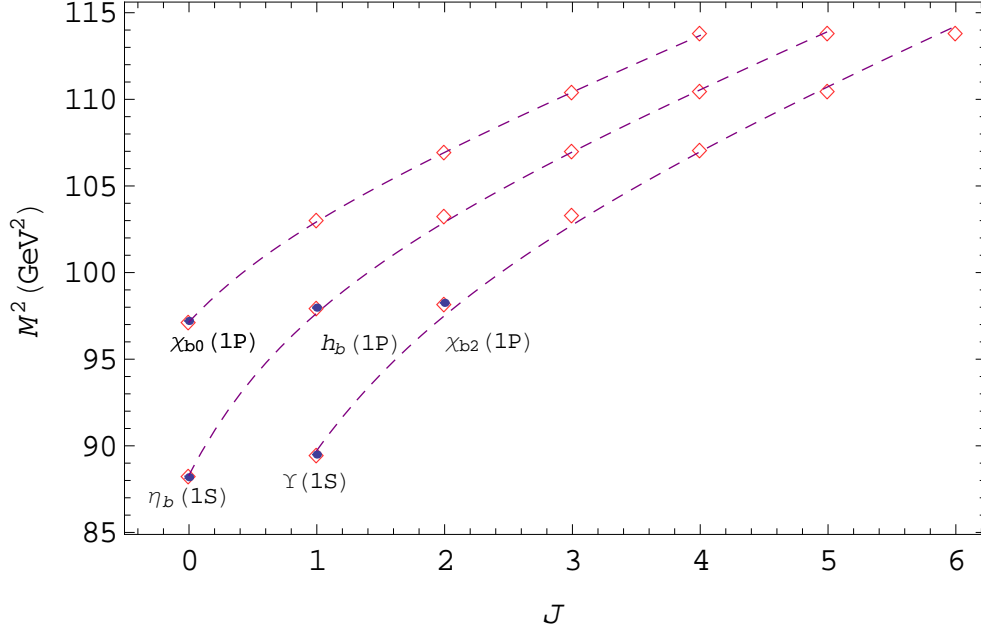


FIG. 6: Nonlinear Regge trajectories in the  $(J, M^2)$  starting from vector, pseudoscalar and scalar bottomonium states (from bottom to top).

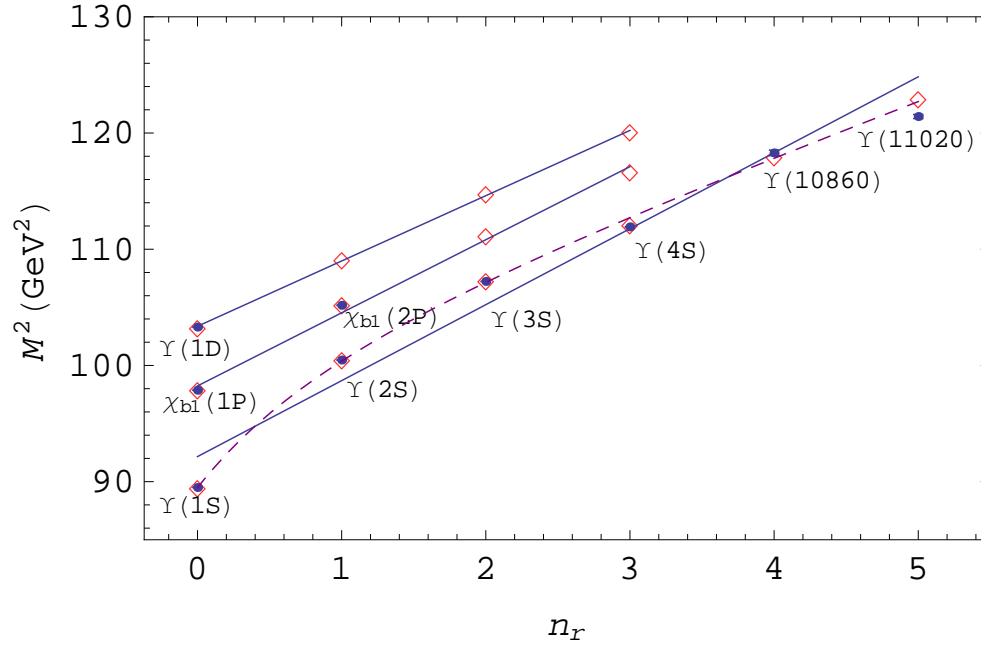


FIG. 7: Same as in Fig. 3 for bottomonium.

$\psi(3770)$  and  $\psi(4160)$  are the  $1^3D_1$  and  $2^3D_1$  states, respectively. These  $\psi$  states fit well to the corresponding Regge trajectories (see Fig. 3). On the other hand, the three new vector states  $X$  are considered as unexpected exotic states (their isospin is not determined experimentally). Indeed, we do not have any  $c\bar{c}$  candidates for these states in Table I. Contrary, in Ref. [12] we have found that these states can be described in our model as

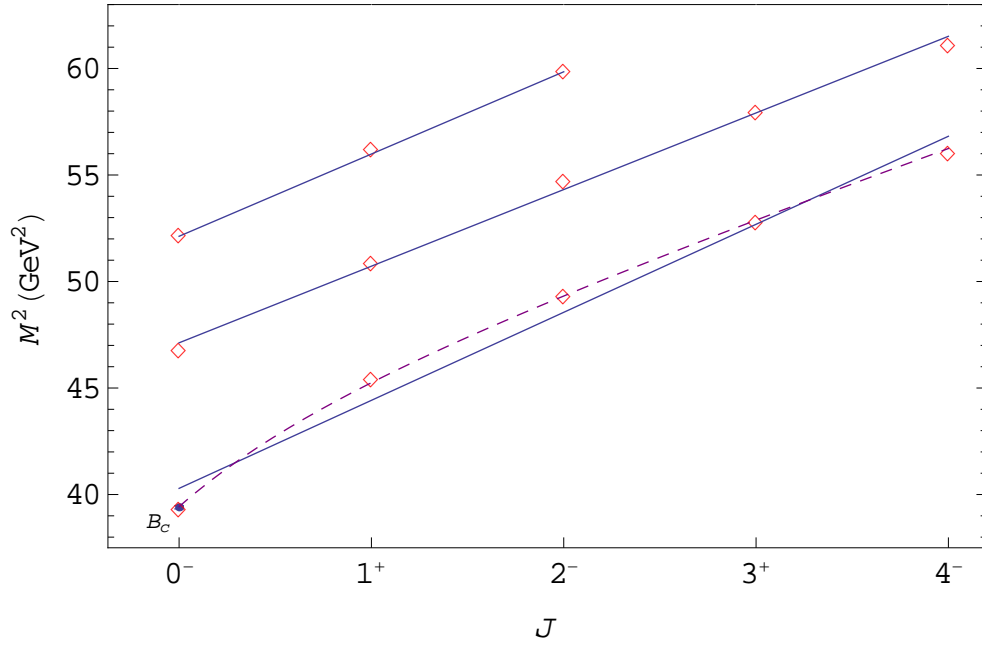


FIG. 8: Same as in Fig. 1 for  $B_c$  meson states with unnatural parity.

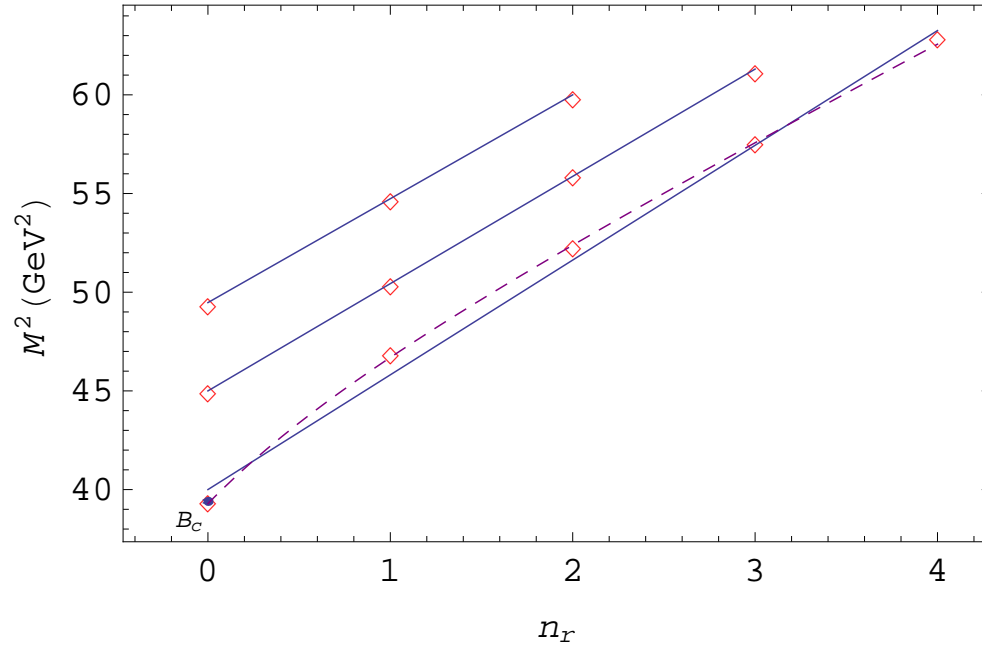


FIG. 9: Same as in Fig. 3 for the  $B_c$  meson.

tetraquarks composed from a diquark and antiquark ( $[cq][\bar{c}\bar{q}]$ ,  $q = u, d$ ). In particular, the  $X(4260)$  and  $X(4660)$  states can be interpreted as the  $1^{--}$  states of such tetraquarks with a scalar diquark  $[cq]_{S=0}$  and scalar antiquark  $[\bar{c}\bar{q}]_{S=0}$  in the relative  $1P$ - and  $2P$ -states and predicted masses 4244 MeV and 4666 MeV, respectively [12]. The  $X(4360)$  can be viewed as the  $1^{--}$  tetraquark with the axial vector diquark  $[cq]_{S=1}$  and axial vector antiquark



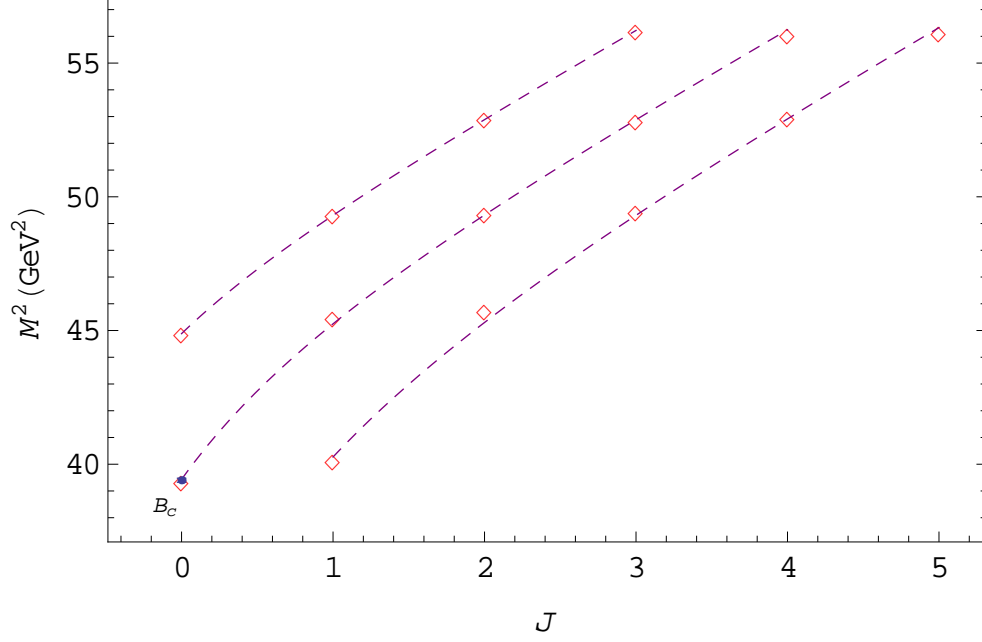


FIG. 10: Same as in Fig. 6 for the  $B_c$  meson.

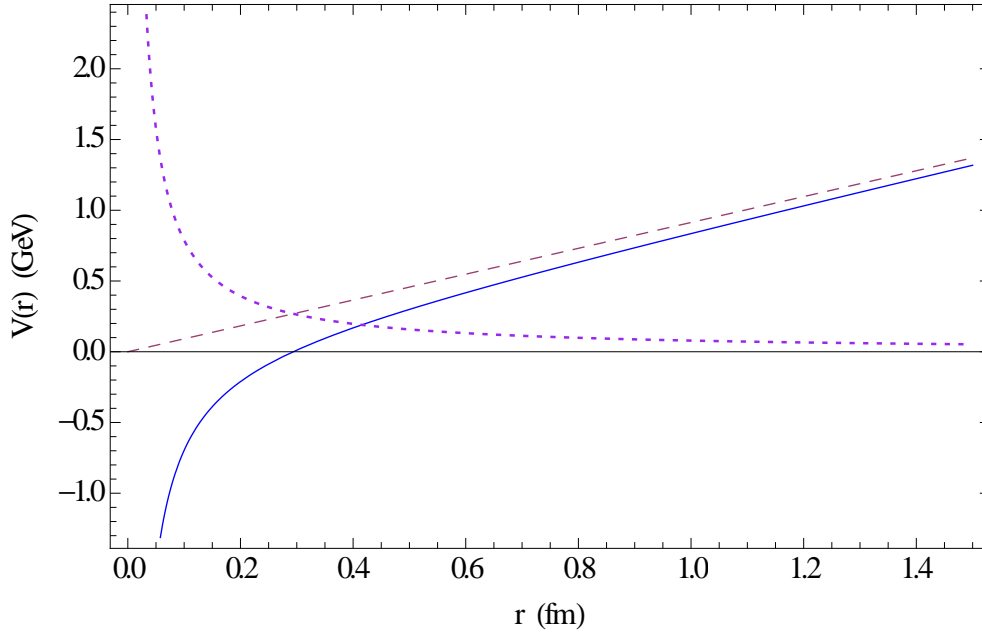


FIG. 11: Static potential of the quark-antiquark interaction (9) without the constant term (solid line). Dashed line shows the linear confining potential contribution, while dotted line corresponds to the modulus of the Coulomb potential.

$[\bar{c}q]_{S=1}$  in the relative  $1P$ -state, which mass is predicted to be 4350 MeV [12].<sup>4</sup>

<sup>4</sup> Note that in Ref. [33] a different prescription for these states is used:  $X(4260)$ ,  $X(4360)$ ,  $\psi(4415)$  and  $X(4660)$  are assigned to  $4S$ ,  $3D$ ,  $5S$  and  $6S$  charmonium  $c\bar{c}$  states. This leads the authors to the conclusion

TABLE IV: Fitted parameters of the  $(J, M^2)$  parent and daughter Regge trajectories for heavy quarkonia and  $B_c$  mesons with natural and unnatural parity.

Trajectory	natural parity		unnatural parity	
	$\alpha$ (GeV $^{-2}$ )	$\alpha_0$	$\alpha$ (GeV $^{-2}$ )	$\alpha_0$
$c\bar{c}$	$J/\psi$		$\eta_c$	
parent	$0.436 \pm 0.014$	$-3.31 \pm 0.22$	$0.416 \pm 0.021$	$-3.90 \pm 0.31$
first daughter	$0.488 \pm 0.011$	$-5.63 \pm 0.18$	$0.479 \pm 0.015$	$-6.36 \pm 0.24$
second daughter	$0.431 \pm 0.036$	$-6.08 \pm 0.68$	$0.414 \pm 0.050$	$-6.66 \pm 0.92$
$c\bar{c}$	$\chi_{c0}$		$\chi_{c1}$	
parent	$0.431 \pm 0.016$	$-5.07 \pm 0.25$	$0.461 \pm 0.008$	$-4.66 \pm 0.12$
daughter	$0.493 \pm 0.031$	$-7.41 \pm 0.53$	$0.456 \pm 0.006$	$-5.83 \pm 0.11$
$b\bar{b}$	$\Upsilon$		$\eta_b$	
parent	$0.212 \pm 0.022$	$-18.5 \pm 2.3$	$0.184 \pm 0.024$	$-16.7 \pm 2.5$
first daughter	$0.246 \pm 0.014$	$-23.8 \pm 1.5$	$0.234 \pm 0.016$	$-23.5 \pm 1.7$
second daughter	$0.262 \pm 0.010$	$-27.1 \pm 1.1$	$0.248 \pm 0.014$	$-26.5 \pm 1.6$
third daughter	$0.246 \pm 0.027$	$-26.6 \pm 3.1$	$0.241 \pm 0.026$	$-27.0 \pm 3.0$
$b\bar{b}$	$\chi_{b0}$		$\chi_{b1}$	
parent	$0.228 \pm 0.021$	$-22.3 \pm 2.2$	$0.239 \pm 0.018$	$-22.5 \pm 1.9$
daughter	$0.254 \pm 0.009$	$-26.7 \pm 1.0$	$0.267 \pm 0.006$	$-27.1 \pm 0.7$
$b\bar{c}$	$B_c^*$		$B_c$	
parent	$0.254 \pm 0.018$	$-9.38 \pm 0.88$	$0.242 \pm 0.019$	$-9.75 \pm 0.95$
first daughter	$0.291 \pm 0.008$	$-12.8 \pm 0.4$	$0.278 \pm 0.009$	$-13.1 \pm 0.5$
second daughter	$0.270 \pm 0.010$	$-13.3 \pm 0.4$	$0.259 \pm 0.007$	$-13.5 \pm 0.4$
$b\bar{c}$	$B_{c0}$		$B_{c1}$	
parent	$0.265 \pm 0.013$	$-12.0 \pm 0.6$	$0.285 \pm 0.007$	$-13.0 \pm 0.4$
daughter	$0.275 \pm 0.014$	$-13.9 \pm 0.8$	$0.298 \pm 0.008$	$-15.3 \pm 0.4$

The three vector bottomonium states,  $\Upsilon(10580)$ ,  $\Upsilon(10860)$  and  $\Upsilon(11020)$ , observed above open bottom threshold [1], are rather well described in our model as  $4^3S_1$ ,  $5^3S_1$  and  $6^3S_1$  states (see Table II). The mass of  $\Upsilon(11020)$  being somewhat higher than the experimental value. They fit to the corresponding Regge trajectory in Fig. 7.

The only experimentally established  $2P$  charmonium state is  $\chi_{c2}(2P)$  which mass is predicted slightly higher (by about 20 MeV) in our model. From Table I we see that the exotic state  $X(3872)$  cannot be described as the  $1^{++} 2^3P_1 c\bar{c}$  state or the  $2^{-+} 1^1D_2 c\bar{c}$  state. If this state belonged to either  $2P$  or  $1D$  multiplets, this could signal a large fine splitting in these multiplets, since the  $X(3872)$  mass is 55 MeV below  $\chi_{c2}(2P)$  and 100 MeV above  $\psi(3770)$ . As we see from Table I, our model does not support such large fine splittings. In Ref. [11, 12] we argued that  $X(3872)$  can be considered as the  $1^{++}$  ground state tetraquark, composed from the scalar and axial vector diquark and antidiquark ( $([cq]_{S=0}[\bar{c}\bar{q}]_{S=1} + [cq]_{S=1}[\bar{c}\bar{q}]_{S=0})/\sqrt{2}$ ), which mass is predicted to be 3871 MeV.

---

that the quark interaction potential should be screened at large distances.

TABLE V: Fitted parameters of the  $(n_r, M^2)$  Regge trajectories for heavy quarkonia and  $B_c$  mesons.

Meson	$\beta$ (GeV $^{-2}$ )	$\beta_0$	Meson	$\beta$ (GeV $^{-2}$ )	$\beta_0$
$c\bar{c}$			$c\bar{c}$		
$\eta_c$	$0.287 \pm 0.011$	$-2.62 \pm 0.18$	$J/\psi$	$0.297 \pm 0.010$	$-2.89 \pm 0.16$
$\chi_{c0}$	$0.288 \pm 0.003$	$-3.34 \pm 0.06$	$\chi_{c1}$	$0.301 \pm 0.011$	$-3.67 \pm 0.19$
$\chi_{c2}$	$0.301 \pm 0.011$	$-3.76 \pm 0.019$	$h_c$	$0.298 \pm 0.010$	$-3.68 \pm 0.17$
$\psi(^3D_1)$	$0.325 \pm 0.006$	$-4.62 \pm 0.11$	$\psi(^3D_2)$	$0.315 \pm 0.003$	$-4.53 \pm 0.06$
$\psi(^3D_3)$	$0.311 \pm 0.002$	$-4.53 \pm 0.04$	$\psi(^1D_2)$	$0.317 \pm 0.003$	$-4.53 \pm 0.06$
$b\bar{b}$			$b\bar{b}$		
$\eta_b$	$0.151 \pm 0.013$	$-13.7 \pm 1.4$	$\Upsilon$	$0.153 \pm 0.012$	$-14.1 \pm 1.3$
$\chi_{b0}$	$0.158 \pm 0.008$	$-15.4 \pm 0.9$	$\chi_{b1}$	$0.159 \pm 0.007$	$-15.7 \pm 0.8$
$\chi_{b2}$	$0.161 \pm 0.007$	$-15.9 \pm 0.7$	$h_b$	$0.161 \pm 0.007$	$-15.8 \pm 0.8$
$\Upsilon(^3D_1)$	$0.178 \pm 0.002$	$-18.4 \pm 0.3$	$\Upsilon(^3D_2)$	$0.178 \pm 0.002$	$-18.4 \pm 0.3$
$\Upsilon(^3D_3)$	$0.178 \pm 0.003$	$-18.4 \pm 0.3$	$\Upsilon(^1D_2)$	$0.178 \pm 0.002$	$-18.4 \pm 0.3$
$b\bar{c}$			$b\bar{c}$		
$B_c$	$0.172 \pm 0.008$	$-6.88 \pm 0.39$	$B_c^*$	$0.175 \pm 0.008$	$-7.15 \pm 0.39$
$B_{c0}$	$0.184 \pm 0.001$	$-8.28 \pm 0.07$	$B_{c2}$	$0.185 \pm 0.001$	$-8.48 \pm 0.07$
$B_c(^3D_1)$	$0.190 \pm 0.002$	$-9.40 \pm 0.12$	$B_c(^3D_2)$	$0.188 \pm 0.002$	$-9.27 \pm 0.11$

TABLE VI: Mean square radii  $\sqrt{\langle r^2 \rangle}$  for the spin-singlet ground and excited states of charmonia,  $B_c$  mesons and bottomonia (in fm).

State	$\sqrt{\langle r^2 \rangle}_\psi$	$\sqrt{\langle r^2 \rangle}_{B_c}$	$\sqrt{\langle r^2 \rangle}_\Upsilon$
$1S$	0.37	0.33	0.22
$1P$	0.59	0.53	0.41
$2S$	0.71	0.63	0.50
$1D$	0.74	0.67	0.54
$2P$	0.87	0.79	0.65
$1F$	0.87	0.79	0.65
$3S$	0.94	0.87	0.72
$1G$	0.98	0.89	0.75
$2D$	0.99	0.90	0.76
$1H$	1.08	0.99	0.85
$3P$	1.09	0.99	0.84
$2F$	1.09	0.99	0.85
$4S$	1.16	1.05	0.90
$3D$	1.18	1.08	0.94
$4P$	1.26	1.16	1.01
$5S$	1.32	1.21	1.07
$6S$	1.46		1.22

TABLE VII: Fitted parameters of the nonlinear Regge trajectories for heavy quarkonia and  $B_c$  mesons.

Meson	$\gamma$ (GeV <sup>-2</sup> )	$\gamma_0$	$\gamma_1$	$\tau$ (GeV <sup>-2</sup> )	$\tau_0$	$\tau_1$
$\Upsilon$	0.33	32.2	32.3	0.22	22.2	10.1
$\eta_b$	0.33	32.9	15.0			
$\chi_{b0}$	0.33	33.7	6.57			
$B_c^*$	0.32	13.3	12.5	0.21	9.25	4.00
$B_c$	0.32	14.2	6.21			
$B_{c0}$	0.32	15.1	2.99			
$J/\psi$	0.48	4.25	5.47	0.31	3.19	0.82
$\eta_c$	0.48	5.19	3.56			

As we see from Table I, the  $X(4160)$  and  $X(4350)$  can be attributed from the point of view of the mass value and charge parity  $C = +$  to the pseudo tensor  $2^{-+}$  spin-singlet  $2^1D_2$  and tensor  $2^{++}$  spin-triplet  $3^3P_2$  charmonium states, respectively. They fit well to the corresponding Regge trajectories in Figs. 1-3.

The  $X(4140)$  state, observed by CDF in  $B^+ \rightarrow K^+ \phi J/\psi$  decays [34], can correspond in our model to the scalar  $0^{++}$  charmed-strange diquark-antidiquark  $[cs]_{S=1}[\bar{c}\bar{s}]_{S=1}$  ground state, which predicted mass is 4110 MeV, or the axial vector  $1^{++}$  one ( $[cs]_{S=0}[\bar{c}\bar{s}]_{S=1} + [cs]_{S=1}[\bar{c}\bar{s}]_{S=0}/\sqrt{2}$ ) with calculated mass 4113 MeV [11, 12].

Two of the three charmonium-like charged  $X^\pm$  states reported by Belle [35], which are explicitly exotic, can be interpreted in our model as tetraquark states. We do not have tetraquark candidates for the  $X(4040)^+$  structure, while the  $X(4250)^+$  can be considered as the charged partner of the  $1^- 1P$  state  $[cu]_{S=0}[\bar{c}\bar{d}]_{S=0}$  or as the  $0^- 1P$  state of the ( $[cu]_{S=0}[\bar{c}\bar{d}]_{S=1} + [cu]_{S=1}[\bar{c}\bar{d}]_{S=0}/\sqrt{2}$ ) tetraquark with predicted masses 4244 MeV and 4267 MeV, respectively [12]. The  $X(4430)^+$  could be the first radial ( $2S$ ) excitation of the  $1^+ X(3872)$  tetraquark or the  $0^+ 2S [cu]_{S=1}[\bar{c}\bar{d}]_{S=1}$  tetraquark, which have very close masses 4431 MeV and 4434 MeV [12].

Very recently the Belle Collaboration [36] reported the observation of two charged bottomonium-like resonances, the  $Z_b(10610)$  and  $Z_b(10650)$ , in the  $\pi^\pm \Upsilon$  and  $\pi^\pm h_b$  mass spectra close to the open-bottom ( $B\bar{B}^*$  and  $B^*\bar{B}^*$ ) production thresholds. The analysis of the charged pion angular distributions favours a  $J^P = 1^+$  spin-parity assignment for both states [36]. In this mass region we do not have any bottom diquark-antidiquark tetraquarks with such quantum numbers [12]. The possible interpretations of these exotic bottomonium-like states are discussed in Ref. [15].

As we see, a consistent picture of the excited quarkonium states emerges in our model. All well-established states and most of the states, which need additional experimental confirmation, can be interpreted as excited quarkonium or diquark-antidiquark tetraquark states.

## V. CONCLUSIONS

The mass spectra of charmonia, bottomonia and  $B_c$  mesons were calculated in the framework of the QCD-motivated relativistic quark model based on the quasipotential approach. Highly radially and orbitally excited quarkonium states were considered. To achieve this

goal, we treated the dynamics of heavy quarks in quarkonia completely relativistically without application of the nonrelativistic  $v^2/c^2$  expansion. The known one-loop radiative corrections were also taken into account in order to improve the agreement with experiment. The comparison of new results with the previous consideration within the  $v^2/c^2$  expansion [7] indicates that relativistic effects become significant with the increase of the excitation and are particularly important for charmonium.

On this basis, the Regge trajectories of heavy quarkonia were constructed both in the  $(J, M^2)$  and  $(n_r, M^2)$  planes. A different behaviour of these trajectories was observed for parent and daughter trajectories. All daughter trajectories turn out to be almost linear and parallel, while parent trajectories exhibit some nonlinearity. Such nonlinearity occurs only in the vicinity of ground states and few lowest excitations and is mostly pronounced for bottomonia. For charmonia this nonlinearity is only marginal, and its account does not significantly improve the fit. It was shown that the masses of the excited states of heavy quarkonia are determined by the average distances between quarks larger than 0.5 fm, where the linear confining part of the quark-antiquark interaction dominates. This leads to the emergence of almost linear Regge trajectories. On the other hand, a few lowest states have average sizes smaller than 0.5 fm and fall in the region, where both the Coulomb and confining potentials play an important role. As a result, the parent Regge trajectories exhibit a certain nonlinearity in this region. The parameters (slopes, intercepts and nonlinearity) of both linear and nonlinear Regge trajectories were determined. They were compared to the slopes of the linear Regge trajectories of light [8] and heavy-light [25] mesons calculated previously. It was found that the slope of the meson Regge trajectory is mainly determined by the mass of the heaviest quark  $m_Q$ .

A detailed comparison of the calculated heavy quarkonium masses with available experimental data was carried out. It was found that all data for the states below open flavour production threshold are well reproduced in our model: the difference between predicted and measured masses does not exceed a few MeV. For higher excited states, which are above this threshold, most of the well-established conventional states are also well described by our approach, the difference between theory and experiment being somewhat larger, but still within 20 MeV. It was shown that these states fit well to the corresponding Regge trajectories. Other states, which have unexpected properties and are therefore believed to have an exotic origin, were also discussed. As it was shown in our previous calculation [11, 12], most of these states can be described as diquark-antidiquark tetraquarks. Therefore we have a self-consistent picture of the heavy quarkonium spectra. Future experimental studies of the yet unobserved conventional quarkonium states and a clarification of the nature and quantum numbers of the exotic quarkonium-like states will provide a further test of our model.

### Acknowledgments

The authors are grateful to M. Müller-Preussker, V. Matveev, V. Savrin and M. Wagner for support and discussions. One of us (V.O.G.) thanks the particle theory group at Humboldt University for kind hospitality. V.O.G. gratefully acknowledges the financial support

by Deutscher Akademischer Austauschdienst (DAAD).

- 
- [1] K. Nakamura *et al.* (Particle Data Group), J. Phys. G **37**, 075021 (2010) and 2011 partial update for the 2012 edition.
  - [2] N. Brambilla *et al.*, Eur. Phys. J. C **71**, 1534 (2011).
  - [3] E. Klempt and A. Zaitsev, Phys. Rept. **454**, 1 (2007).
  - [4] A. A. Alves *et al.* [LHCb Collaboration], JINST **3**, S08005 (2008).
  - [5] L. L. Gioi, arXiv:1109.3398 [hep-ex].
  - [6] LHCb Collaboration, LHCb-CONF-2011-027 (2011).
  - [7] D. Ebert, R.N. Faustov and V.O. Galkin, Phys. Rev. D **67**, 014027 (2003).
  - [8] D. Ebert, R. N. Faustov and V. O. Galkin, Phys. Rev. D **79**, 114029 (2009).
  - [9] D. Ebert, R. N. Faustov and V. O. Galkin, Mod. Phys. Lett. A **20**, 1887 (2005); Eur. Phys. J. C **47**, 745 (2006).
  - [10] S. Gupta and S. F. Radford, Phys. Rev. D **24**, 2309 (1981); *ibid.* **25**, 3430 (1982); S. Gupta, S. F. Radford and W. W. Repko, Phys. Rev. D **26**, 3305 (1982); J. Pantaleone, S.-H. H. Tye and Y. J. Ng, Phys. Rev. D **33**, 777 (1986).
  - [11] D. Ebert, R. N. Faustov and V. O. Galkin, Phys. Lett. B **634**, 214 (2006).
  - [12] D. Ebert, R. N. Faustov and V. O. Galkin, Eur. Phys. J. C **58**, 399 (2008); Mod. Phys. Lett. A **24**, 567 (2009).
  - [13] S. Godfrey and S. L. Olsen, Ann. Rev. Nucl. Part. Sci. **58**, 51 (2008).
  - [14] E. S. Swanson, Phys. Rept. **429**, 243 (2006).
  - [15] A. Ali, arXiv:1108.2197 [hep-ph].
  - [16] S. S. Gershtein, A. K. Likhoded and A. V. Luchinsky, Phys. Rev. D **74**, 016002 (2006).
  - [17] K. W. Wei and X. H. Guo, Phys. Rev. D **81**, 076005 (2010).
  - [18] A. M. Badalian, Phys. Atom. Nucl. **74**, 1375 (2011).
  - [19] G. S. Bali, S. Collins and C. Ehmman, arXiv:1110.2381 [hep-lat].
  - [20] D. Ebert, V. O. Galkin and R. N. Faustov, Phys. Rev. D **57**, 5663 (1998) [Erratum-*ibid.* D **59**, 019902 (1999)].
  - [21] N. Brambilla, P. Consoli and G. M. Prosperi, Phys. Rev. D **50**, 578 (1994).
  - [22] A. H. Hoang and A. V. Manohar, Phys. Lett. B **491**, 101 (2000); M. Melles, Phys. Rev. D **62**, 074019 (2000); N. Brambilla, Y. Sumino and A. Vairo, Phys. Rev. D **65**, 034001 (2002).
  - [23] D. Ebert, R. N. Faustov and V. O. Galkin, Phys. Rev. D **66**, 037501 (2002).
  - [24] M. N. Sergeenko, Z. Phys. C **64**, 315 (1994).
  - [25] D. Ebert, R. N. Faustov and V. O. Galkin, Eur. Phys. J. C **66**, 197 (2010).
  - [26] E. Eichten, K. Gottfried, T. Kinoshita, K. D. Lane and T. M. Yan, Phys. Rev. D **17**, 3090 (1978) [Erratum-*ibid.* D **21**, 313 (1980)].
  - [27] T. Barnes and E. S. Swanson, Phys. Rev. C **77**, 055206 (2008).
  - [28] B. Aubert *et al.* [BABAR Collaboration], Phys. Rev. Lett. **101**, 071801 (2008); Phys. Rev. Lett. **103**, 161801 (2009); G. Bonvicini *et al.* [CLEO Collaboration], Phys. Rev. D **81**, 031104 (2010).
  - [29] I. Adachi *et al.* [Belle Collaboration], arXiv:1110.3934 [hep-ex].
  - [30] B. A. Kniehl, A. A. Penin, A. Pineda, V. A. Smirnov and M. Steinhauser, Phys. Rev. Lett. **92**, 242001 (2004) [Erratum-*ibid.* **104**, 199901 (2010)]; S. Recksiegel and Y. Sumino, Phys. Lett. B **578**, 369 (2004).

- [31] M. Andreotti *et al.* [Fermilab E835 Collaboration], Phys. Rev. D **72**, 032001 (2005); S. Dobbs *et al.* [CLEO Collaboration], Phys. Rev. Lett. **101**, 182003 (2008); M. Ablikim *et al.* [The BESIII Collaboration], Phys. Rev. Lett. **104**, 132002 (2010).
- [32] J. P. Lees [The BABAR Collaboration], arXiv:1102.4565 [hep-ex]; I. Adachi *et al.* [Belle Collaboration], arXiv:1103.3419 [hep-ex]; J. P. Lees *et al.* [BABAR Collaboration], Phys. Rev. D **84**, 011104 (2011).
- [33] P. Gonzalez, V. Mathieu and V. Vento, arXiv:1108.2347 [hep-ph].
- [34] T. Aaltonen *et al.* [CDF Collaboration], Phys. Rev. Lett. **102**, 242002 (2009).
- [35] S. K. Choi *et al.* [Belle Collaboration], Phys. Rev. Lett. **100**, 142001 (2008); R. Mizuk *et al.* [Belle Collaboration], Phys. Rev. D **78**, 072004 (2008); Phys. Rev. D **80**, 031104 (2009).
- [36] I. Adachi *et al.* [Belle Collaboration], arXiv:1105.4583 [hep-ex]; A. Bondar *et al.* [Belle Collaboration], arXiv:1110.2251 [hep-ex].